

PAPER

Simultaneous reconstruction of shape and generalized impedance functions in electrostatic imaging

To cite this article: Fioralba Cakoni *et al* 2014 *Inverse Problems* **30** 105009

View the [article online](#) for updates and enhancements.

Related content

- [Integral equation methods for the inverse obstacle problem with generalized impedance boundary condition](#)
Fioralba Cakoni and Rainer Kress
- [Integral equations for shape and impedance reconstruction in corrosion detection](#)
Fioralba Cakoni, Rainer Kress and Christian Schuft
- [Nonlinear integral equations for the inverse electrical impedance problem](#)
Harry Eckel and Rainer Kress

Recent citations

- [Shape Sensitivity Analysis for Elastic Structures with Generalized Impedance Boundary Conditions of the Wentzell Type—Application to Compliance Minimization](#)
Fabien Caubet *et al*
- [Rainer Kress](#)
- [Recovering the boundary corrosion from electrical potential distribution using partial boundary data](#)
Gen Nakamura and Jijun Liu



IOP | ebooks™

Bringing you innovative digital publishing with leading voices to create your essential collection of books in STEM research.

Start exploring the collection - download the first chapter of every title for free.

Simultaneous reconstruction of shape and generalized impedance functions in electrostatic imaging

Fioralba Cakoni¹, Yuqing Hu² and Rainer Kress³

¹ Department of Mathematical Sciences, University of Delaware, Newark, Delaware 19716, USA

² Department of Mathematics, Southeast University, Nanjing 211189, People's Republic of China

³ Institut für Numerische und Angewandte Mathematik, Universität Göttingen, Göttingen, Germany

E-mail: cakoni@math.udel.edu, huyuqing.good@163.com and kress@math.uni-goettingen.de

Received 11 June 2014, revised 6 September 2014

Accepted for publication 8 September 2014

Published 30 September 2014

Abstract

Determining the geometry and the physical nature of an inclusion within a conducting medium from voltage and current measurements on the accessible boundary of the medium can be modeled as an inverse boundary value problem for the Laplace equation subject to appropriate boundary conditions on the inclusion. We continue the investigations on the particular inverse problem with a generalized impedance condition started in Cakoni and Kress (2013 *Inverse Problems* **29** 015005) by presenting an inverse algorithm for the simultaneous reconstruction of both the shape of the inclusion and the two impedance functions via a boundary integral equation approach. In addition to describing the reconstruction algorithm and illustrating its feasibility by numerical examples we also provide some extensions to the uniqueness results in Cakoni and Kress (2013 *Inverse Problems* **29** 015005).

Keywords: inverse boundary value problem, integral equations, generalized impedance boundary condition, iterative method, uniqueness

(Some figures may appear in colour only in the online journal)

1. Introduction

Electrostatic imaging can be modeled in terms of inverse problems for the Laplace equation in a bounded domain subject to an appropriate boundary condition. In this paper we will continue our investigations started in [7] for a generalized impedance boundary condition. For this we assume that Ω is a doubly connected bounded domain in \mathbb{R}^2 with boundary $\partial\Omega$ that consists of two disjoint C^2 smooth closed Jordan curves Γ_m and Γ_c such that $\partial\Omega := \Gamma_m \cup \Gamma_c$ and Γ_c is contained in the interior of Γ_m . Here, Γ_c stands for a corroded surface to be evaluated and Γ_m stands for the measurement surface. We denote by Ω_c and Ω_m the bounded domains with boundary Γ_c and Γ_m , respectively. By ν we denote the unit normal vector to Γ_c and to Γ_m that is directed into the exterior of Ω_c and the exterior of Ω_m , respectively. (Note, that the orientation of the normal vector on Γ_c in this paper differs from that in [7].) We assume that the electrostatic potential u satisfies

$$\Delta u = 0 \quad \text{in } \Omega \quad (1.1)$$

subject to the generalized impedance boundary condition

$$\frac{\partial u}{\partial \nu} + \frac{d}{ds} \mu \frac{du}{ds} - \lambda u = 0 \quad \text{on } \Gamma_c \quad (1.2)$$

in terms of arc length s on Γ_c , where $\lambda \in C^1(\Gamma_c)$ is non-negative and not identically zero and $\mu \in C^1(\Gamma_c)$ is positive. The inverse problem is to determine both the shape Γ_c and the impedance functions λ and μ from a knowledge of a (small) finite number of Cauchy pairs

$$f := u|_{\Gamma_m} \quad \text{and} \quad g := \frac{\partial u}{\partial \nu} \Big|_{\Gamma_m}$$

for solutions u of (1.1) and (1.2), i.e., from applied voltage and measured corresponding current densities on Γ_m .

As demonstrated among others in [1, 11, 13, 14], the generalized impedance condition (1.2) models complex materials with coated or corroded surfaces much more accurate than the traditional classical impedance condition, i.e., the case where $\mu = 0$. Hence our inverse generalized impedance problem for both the shape and the impedance functions serves as a model problem for the identification and characterization of complex targets such as coated objects via electric imaging applications in non-destructive testing. We emphasize that our reconstruction algorithm carries over to the Helmholtz equation, i.e., to inverse scattering, by just substituting the appropriate fundamental solution.

In [7] two of us settled existence and well-posedness for the direct problem with the generalized impedance condition by boundary integral equations via a single-layer potential approach involving a hypersingular operator. In particular, given $f \in H^{3/2}(\Gamma_m)$ there exists a unique harmonic function $u \in H^2(\Omega)$ satisfying the generalized impedance condition (1.2) on Γ_c and the Dirichlet boundary condition $u = f$ on Γ_m . We further provided and tested a numerical algorithm by a collocation method based on trigonometric polynomial approximations and trigonometric numerical differentiation. For a corresponding convergence analysis we refer to [19].

For the inverse problem, in [7] we obtained a uniqueness result for recovering both impedance functions λ and μ for a known boundary Γ_c of the inclusion together with a reconstruction algorithm based on the uniqueness proof requiring three Cauchy pairs. Further, in the spirit of the method proposed by Kress and Rundell [20] for an inverse Dirichlet problem, from Green's representation theorem for harmonic functions we derived a system of two nonlinear boundary integral equations on Γ_c and Γ_m for four unknowns, namely Γ_c , λ and μ together with the unknown Dirichlet trace $u|_{\Gamma_c}$ as a slip-variable. Adopting the approach of

Johansson and Sleeman [15] for an inverse scattering problem and for a corrosion detection problem [6], for known impedance functions λ and μ we proposed and tested an inverse method for iteratively reconstructing the shape of Γ_c . Given an approximation for Γ_c , this algorithm solves the well-posed integral equation on Γ_c for $\varphi := u|_{\Gamma_c}$ and then, keeping φ fixed obtains an update for Γ_c by linearizing the integral equation on Γ_m with respect to Γ_c .

In the main part of this paper we follow the ideas in [9, 20] more closely and simultaneously linearize both equations with respect to the four unknowns Γ_c , λ , μ and $u|_{\Gamma_c}$. Of course, since two equations will not suffice to determine four unknowns and since each additional Cauchy pair generates an additional unknown by its Dirichlet trace on Γ_c we will need at least three Cauchy pairs to successfully perform this algorithm. This heuristic analysis is also supported by the fact that we need at least two Cauchy pairs for recovering λ and μ for a known shape Γ_c , see the remark after theorem 2.1. For related work in inverse scattering we refer to [3–5].

The plan of the paper is as follows. Section 2 is devoted to some considerations on the uniqueness issue for the inverse problem. In particular, this includes unique reconstruction of both Γ_c and the impedance functions λ and μ from all Cauchy data on Γ_m . We note that although this uniqueness result can be extended to the case where the Cauchy data are known only on part of Γ_m our reconstruction does not have an immediate extension to this case since it is based on the use of Green's representation formula. We then proceed in section 3 with the presentation of the inverse algorithm for the simultaneous reconstruction of the shape Γ_c and the impedance functions λ and μ via linearization and iteration. In section 4 we will prove a corresponding local uniqueness result and in the final section 5 we will provide numerical examples illustrating the feasibility of the inverse algorithm.

2. Uniqueness revisited

In [7] it is shown that three Cauchy pairs with linearly independent Dirichlet data uniquely determine the impedance functions λ and μ provided the shape Γ_c is known. Picking up on ideas in [2, 21], we show that two Cauchy pairs suffice for uniqueness provided the Dirichlet data of one of them does not change sign on Γ_m .

Theorem 2.1. *Assume that Γ_c is C^4 and let $f_1 \geq 0$ and f_2 be linearly independent. Then the two Cauchy pairs (f_1, g_1) and (f_2, g_2) for the solutions u_1 and u_2 of the generalized impedance problem (1.1)–(1.2) uniquely determine the coefficient functions λ and μ .*

Proof. From the proof of theorem 3.3 in [7] we recall that the solution to the generalized impedance problem is of class C^2 up to the boundary Γ_c provided the latter is C^4 smooth. Hence, we can apply Hopf's lemma (see e.g. [12]). Now assume that the minimum of u_1 over Γ_c is not positive. Clearly each $x_{\min} \in \Gamma_c$, where this minimum is attained also is a minimal point of u_1 over $\bar{\Omega}$. Then we have that

$$\frac{du_1}{ds}(x_{\min}) = 0 \quad \text{and} \quad \frac{d^2u_1}{ds^2}(x_{\min}) \geq 0$$

and therefore

$$\frac{\partial u_1}{\partial \nu}(x_{\min}) \leq 0$$

as consequence of the generalized impedance condition (1.2). However, this is a contradiction to Hopf's lemma. Hence, $u_1 > 0$ on Γ_c .

This now can be used to rewrite the Wronskian $W(u_1, u_2)$ for the trace of u_1 and u_2 on Γ_c in the form

$$W(u_1, u_2) = u_1^2 \frac{d}{ds} \left(\frac{u_2}{u_1} \right)$$

which implies that W has at least one zero on Γ_c . Multiplying the impedance condition for u_1 by u_2 and the impedance condition of u_2 by u_1 and subtract as in [7, theorem 3.1] we obtain

$$\frac{d}{ds} \mu W(u_1, u_2) = u_2 \frac{\partial u_1}{\partial \nu} - u_1 \frac{\partial u_2}{\partial \nu} \quad \text{on } \Gamma_c.$$

From this, μ is now uniquely determined by integration since the zero of $W(u_1, u_2)$ forces the constant occurring in the integration to be zero.

Once we know μ , the remaining function λ can be obtained from the impedance condition (1.2) for u_1 which does not vanish on Γ_c . \square

For constants λ and μ the function

$$u(x) = 1 + \frac{\rho\lambda}{1 - \lambda\rho \ln \rho} \ln |x|$$

satisfies (1.2) in $\Omega = \{x \in \mathbb{R}^2 : \rho < |x| < 1\}$ for any value of μ . Hence, in view of the preceding theorem, at least two Cauchy pairs are required to recover both impedance functions.

Motivated by the above, we also tried to extend Bacchelli's [2] ideas to obtain a uniqueness result for both the shape and the impedance functions using finitely many Cauchy pairs. However, so far we did not succeed along these lines. Therefore, here we include a uniqueness result based on infinitely many Cauchy pairs.

To this end we need to introduce also solutions to the generalized impedance problem with singularities that we can move towards the interior boundary Γ_c . For a discussion of singularities it is advantageous to have the well-posedness of the generalized impedance problem also available in a Hölder space setting. To abbreviate notations, we define the generalized impedance operator $G : H^2(\Omega) \rightarrow H^{-1/2}(\Gamma_c)$ by

$$Gu := \frac{\partial u}{\partial \nu} + \frac{d}{ds} \mu \frac{du}{ds} - \lambda u.$$

The analysis in [7] for the direct problem can also be performed by considering the boundary integral equation arising from the single-layer potential approach as an equation for an operator from $C^{1,\alpha}(\Gamma_m) \times C^{1,\alpha}(\Gamma_c)$ into $C^{2,\alpha}(\Gamma_m) \times C^{0,\alpha}(\Gamma_c)$. From this it can be seen that for $h \in C^{0,\alpha}(\Gamma_c)$ the unique harmonic function $u \in H^2(\Omega)$ satisfying $u = 0$ on Γ_m and $Gu = h$ on Γ_c belongs to $C^{2,\alpha}(\Omega)$ and depends continuously on h , that is,

$$\|u\|_{C^{2,\alpha}(\Omega)} \leq C \|h\|_{C^{0,\alpha}(\Gamma_c)} \quad (2.1)$$

for some constant C depending only on Ω and the impedance functions. For this we need to assume that Γ_c is C^3 smooth (see [16]).

Now, for $z \in \Omega$ let $w_z \in H^2(\Omega)$ be the unique harmonic function satisfying $w_z = 0$ on Γ_m and

$$G(w_z + \Phi(\cdot, z)) = 0 \quad \text{on } \Gamma_c, \quad (2.2)$$

where

$$\Phi(x, y) := \frac{1}{2\pi} \ln \frac{1}{|x - y|}, \quad x \neq y, \quad (2.3)$$

denotes the fundamental solution to the Laplace equation in two dimensions.

Further, for $f \in H^{3/2}(\Gamma_m)$ by writing u_f we indicate the dependence of the solution to (1.1)–(1.2) on the Dirichlet values. In addition, we introduce the unique harmonic function $v_f \in H^2(\Omega_m)$ with Dirichlet values $v_f = f$ on Γ_m and set

$$\tilde{u}_f := u_f - v_f|_{\Omega}.$$

From the double-layer potential approach for the solution to the interior Dirichlet problem and the well-posedness of the corresponding boundary integral equation it can be deduced that for any compact set $M \subset \Omega_m$ the set of harmonic functions

$$\left\{ v_f|_M : f \in H^{3/2}(\Gamma_m) \right\}$$

is dense in $C^2(M)$ (see e.g. [10, theorem 5.26]). Therefore, for any $z \in \Omega$ and any domain D with $\bar{\Omega}_c \subset D$ and $\bar{D} \subset \Omega_m$ such that $z \notin \bar{D}$ we can choose a sequence (f_n) in $H^{3/2}(\Gamma_m)$ such that

$$\left\| v_{f_n} - \Phi(\cdot, z) \right\|_{C^2(\bar{D})} \rightarrow 0, \quad n \rightarrow \infty.$$

By the well-posedness of the inhomogeneous generalized impedance problem this implies that

$$\left\| \frac{\partial}{\partial \nu} [\tilde{u}_{f_n} - w_z] \right\|_{H^{-1/2}(\Gamma_m)} \rightarrow 0, \quad n \rightarrow \infty. \quad (2.4)$$

Theorem 2.2. Assume that Γ_c^1 and Γ_c^2 are two interior boundary curves and λ_1, μ_1 and λ_2, μ_2 two pairs of impedance functions such that for the corresponding solutions u_f^1 and u_f^2 of (1.1)–(1.2) with Dirichlet values f on Γ_m we have that

$$\frac{\partial u_f^1}{\partial \nu} = \frac{\partial u_f^2}{\partial \nu} \quad \text{on } \Gamma_m \quad (2.5)$$

for all $f \in H^{3/2}(\Gamma_m)$. Then $\Gamma_c^1 = \Gamma_c^2$, $\lambda_1 = \lambda_2$ and $\mu_1 = \mu_2$. (Note that it suffices that (2.5) is satisfied on a dense subset of $H^{3/2}(\Gamma_m)$.)

Proof. We indicate the quantities associated with Γ_c^1 and Γ_c^2 by superscripts and denote by $\Omega^{1,2}$ the connected component of $\Omega_m \setminus (\bar{\Omega}_c^1 \cup \bar{\Omega}_c^2)$ that contains Γ_m as part of its boundary. Since $\Omega^{1,2}$ is open, for arbitrary z in $\Omega^{1,2}$ we choose D such that $z \notin \bar{D}$ as well as $\bar{\Omega}_c^1 \subset D$, $\bar{\Omega}_c^2 \subset D$, and $\bar{D} \subset \Omega_m$. Then from (2.4) we can conclude that

$$\frac{\partial w_z^1}{\partial \nu} = \frac{\partial w_z^2}{\partial \nu} \quad \text{on } \Gamma_m \quad (2.6)$$

for all $z \in \Omega^{1,2}$, since from the assumption of the theorem it follows that

$$\frac{\partial \tilde{u}_f^1}{\partial \nu} = \frac{\partial \tilde{u}_f^2}{\partial \nu} \quad \text{on } \Gamma_m$$

for all $f \in H^{3/2}(\Gamma_m)$. By Holmgren's theorem, (2.6) implies $w_z^1 = w_z^2$ in $\Omega^{1,2}$.

Now assume that $\Gamma_c^1 \neq \Gamma_c^2$. Then without loss of generality, there exists $z \in \partial\Omega^{1,2}$ such that $z \in \Gamma_c^1$ and $z \notin \overline{\Omega_c^2}$. In particular we have that

$$z_n := z + \frac{\eta}{n} \nu(z) \in \Omega^{1,2}, \quad n = 1, 2, \dots,$$

for a sufficiently small constant $\eta > 0$. Then, on one hand from the well-posedness (2.1) we observe that $\|G^1 w_{z_n}^2\|_{C^{0,\alpha}(\Gamma_c^1)}$ remains bounded as $n \rightarrow \infty$. On the other hand, because of the boundary condition for $w_{z_n}^1$ we have that

$$\|G^1 w_{z_n}^1\|_{C^{0,\alpha}(\Gamma_c^1)} = \|G^1 \Phi(\cdot, z_n)\|_{C^{0,\alpha}(\Gamma_c^1)} \rightarrow \infty, \quad n \rightarrow \infty.$$

This contradicts $w_{z_n}^1 = w_{z_n}^2$ for all n and therefore $\Gamma_c^1 = \Gamma_c^2$. Then $\lambda_1 = \lambda_2$ and $\mu_1 = \mu_2$ finally follow from theorem 2.1. \square

3. The inverse algorithm

We now proceed with describing the inverse algorithm for a simultaneous reconstruction of the shape of the inclusion and the impedance functions. To this end, in terms of the fundamental solution Φ as given by (2.3) we introduce the single- and double-layer potential operators

$$S_{jk} : H^{-1/2+s}(\Gamma_j) \rightarrow H^{1/2+s}(\Gamma_k) \quad \text{and} \quad K_{jk} : H^{1/2+s}(\Gamma_j) \rightarrow H^{1/2+s}(\Gamma_k)$$

defined by

$$(S_{jk}\varphi)(x) := 2 \int_{\Gamma_j} \Phi(x, y) \varphi(y) ds(y), \quad x \in \Gamma_k, \quad (3.1)$$

and

$$(K_{jk}\varphi)(x) := 2 \int_{\Gamma_j} \frac{\partial \Phi(x, y)}{\partial(y)} \varphi(y) ds(y), \quad x \in \Gamma_k, \quad (3.2)$$

for $j, k = m, c$ and $-1 \leq s \leq 1$. Without loss of generality, we assume that there exists a point x_m in Ω_m such that $|x - x_m| \neq 1$ for all $x \in \Gamma_m$ and a point x_c in Ω_c such that $|x - x_c| \neq 1$ for all $x \in \Gamma_c$. Then theorem 3.16 in [17] guarantees that the single-layer operators $S_{jj} : H^{-1/2}(\Gamma_k) \rightarrow H^{1/2}(\Gamma_k)$ are injective for $j = m, c$.

For a solution $u \in H^2(\Omega)$ to (1.1)–(1.2) with Cauchy data (f, g) on Γ_m we set

$$\varphi := u|_{\Gamma_c}$$

and, by Green's formula we have that

$$u(x) = \int_{\Gamma_c} \left\{ \frac{\partial \Phi(x, y)}{\partial \nu(y)} \varphi(y) + \Phi(x, y) \left(\frac{d}{ds} \mu \frac{d\varphi}{ds} - \lambda \varphi \right) (y) \right\} ds(y) \\ + \int_{\Gamma_m} \left\{ \Phi(x, y) g(y) - \frac{\partial \Phi(x, y)}{\partial \nu(y)} f(y) \right\} ds(y), \quad x \in \Omega. \quad (3.3)$$

Letting x tend to Γ_m and Γ_c from inside Ω , we obtain the integral equations

$$S_{cm} \left(\frac{d}{ds} \mu \frac{d\varphi}{ds} - \lambda \varphi \right) + K_{cm} \varphi = f + K_{mm} f - S_{mm} g \quad (3.4)$$

and

$$S_{cc} \left(\frac{d}{ds} \mu \frac{d\varphi}{ds} - \lambda \varphi \right) - \varphi + K_{cc} \varphi = K_{mc} f - S_{mc} g \quad (3.5)$$

for the four unknowns Γ_c , λ , μ and φ .

Conversely, assume that for a given Cauchy pair (f, g) on Γ_m the curve Γ_c and the functions λ , μ and φ solve the system of integral equations (3.4) and (3.5) and define a function u by the right-hand side of (3.3) for all $x \in \mathbb{R}^2 \setminus \partial\Omega$. Then from the integral equations (3.4) and (3.5) and the jump relations it follows that the limits of u obtained by approaching Γ_c from inside Ω_c and Γ_m from outside Ω_m both vanish. Uniqueness for the interior and exterior Dirichlet problem together with some consideration on the behavior of the single-layer potentials at infinity using our geometric assumption on Γ_c and Γ_m (see [7]) now imply that u vanishes in $\mathbb{R}^2 \setminus \Omega$. Again the jump relations finally yield that the harmonic function u in D has Cauchy data (f, g) on Γ_m , Dirichlet values $u = \varphi$ on Γ_c and satisfies the generalized impedance condition with coefficients λ and μ on Γ_c . Hence we can state the following equivalence (see also [7, theorem 3.2]).

Theorem 3.1. *The inverse problem for shape and impedance is equivalent to solving the system of integral equations (3.4) and (3.5) for Γ_c , λ , μ and φ .*

For an approximate solution of (3.4)–(3.5), following ideas first developed by Kress and Rundell [20], we employ Newton iterations, i.e., given approximations for all four unknowns we linearize both equations with respect to all four unknowns and solve the linearized equations for updating the unknowns.

Since the equations (3.4)–(3.5) are linear with respect to λ , μ and φ , for the linearization we only need to be concerned with the derivatives of the operators with respect to the boundary Γ_c . To this end without much loss of generality we assume that the C^2 -boundaries Γ_j for $j = m, c$ have parametric representations with counter clockwise orientation

$$\Gamma_j = \{z_j(t): t \in [0, 2\pi]\} \quad (3.6)$$

with 2π periodic C^2 smooth functions $z_j: \mathbb{R} \rightarrow \mathbb{R}^2$ such that z_j is injective on $[0, 2\pi)$. In view of (3.1) and (3.2) we introduce parameterized single- and double-layer operators

$$\tilde{S}_{jk} : H_{\text{per}}^{-1/2+s} [0, 2\pi] \rightarrow H_{\text{per}}^{1/2+s} [0, 2\pi] \quad \text{and} \quad \tilde{K}_{jk} : H_{\text{per}}^{1/2+s} [0, 2\pi] \rightarrow H_{\text{per}}^{1/2+s} [0, 2\pi]$$

by

$$\tilde{S}_{jk}(\psi)(t) := \frac{1}{\pi} \int_0^{2\pi} \ln \frac{1}{|z_k(t) - z_j(\tau)|} \psi(\tau) d\tau, \quad t \in [0, 2\pi], \quad (3.7)$$

and

$$\tilde{K}_{jk}(\psi)(t) := \frac{1}{\pi} \int_0^{2\pi} \frac{[z'_j(\tau)]^\perp \cdot [z_k(t) - z_j(\tau)]}{|z_k(t) - z_j(\tau)|^2} \psi(\tau) d\tau, \quad t \in [0, 2\pi], \quad (3.8)$$

for $j, k = m, c$ and $-1 \leq s \leq 1$. Here, we write $a^\perp = (a_2, -a_1)$ for any vector $a = (a_1, a_2)$, that is, a^\perp is obtained by rotating a clockwise by 90° .

For the parameterized versions of the integral equations (3.4) and (3.5) we also introduce transformed impedance functions by

$$\tilde{\lambda} := |z'_c| \lambda \circ z_c \quad \text{and} \quad \tilde{\mu} := \frac{\mu \circ z_c}{|z'_c|}. \quad (3.9)$$

Then, given finitely many Cauchy pairs (f_ℓ, g_ℓ) , $\ell = 1, \dots, p$, the parameterized version of (3.4) and (3.5) becomes

$$\tilde{S}_{cm} \left((\tilde{\mu} \varphi'_\ell)' - \tilde{\lambda} \varphi_\ell \right) + \tilde{K}_{cm} \varphi_\ell = f_\ell + \tilde{K}_{mm} f_\ell - \tilde{S}_{mm} g_\ell \quad (3.10)$$

and

$$\tilde{S}_{cc} \left((\tilde{\mu} \varphi'_\ell)' - \tilde{\lambda} \varphi_\ell \right) - \varphi_\ell + \tilde{K}_{cc} \varphi_\ell = \tilde{K}_{mc} f_\ell - \tilde{S}_{mc} g_\ell \quad (3.11)$$

for $\ell = 1, \dots, p$. Here, for convenience, we identified f_ℓ, g_ℓ and φ_ℓ with $f_\ell \circ z_m, |z'_m| g_\ell \circ z_m$ and $\varphi_\ell \circ z_c$, respectively. The system of $2p$ equations (3.10)–(3.11) needs to be solved for the $p + 3$ unknowns $z_c, \tilde{\lambda}, \tilde{\mu}$ and $\varphi_\ell, \ell = 1, \dots, p$.

The Fréchet derivatives of the operators given by (3.7) and (3.8) with respect to the boundary are obtained by differentiating their kernels with respect to z_c . The derivatives of the single-layer operators are given by

$$\begin{aligned} d\tilde{S}_{cc}[\psi, z_c; \zeta](t) &= -\frac{1}{\pi} \int_0^{2\pi} \frac{[z_c(t) - z_c(\tau)] \cdot [\zeta(t) - \zeta(\tau)]}{|z_c(t) - z_c(\tau)|^2} \psi(\tau) d\tau, \\ d\tilde{S}_{cm}[\psi, z_c; \zeta](t) &= \frac{1}{\pi} \int_0^{2\pi} \frac{[z_m(t) - z_c(\tau)] \cdot \zeta(\tau)}{|z_m(t) - z_c(\tau)|^2} \psi(\tau) d\tau, \\ d\tilde{S}_{mc}[\psi, z_c; \zeta](t) &= -\frac{1}{\pi} \int_0^{2\pi} \frac{[z_c(t) - z_m(\tau)] \cdot \zeta(\tau)}{|z_c(t) - z_m(\tau)|^2} \psi(\tau) d\tau \end{aligned} \quad (3.12)$$

for $t \in [0, 2\pi]$. Note, that the way we set up the parameterized equations we avoided the explicit occurrence of the arc length parameter $|z'_c|$ in the parameterized single-layer operators which simplified the derivatives with respect to z_c . The kernel of $d\tilde{S}_{cc}$ is smooth with diagonal values

$$-\frac{z'_c(t) \cdot \zeta'(t)}{\pi |z'_c(t)|^2}.$$

The derivatives of the double-layer potentials are slightly more involved and given by

$$\begin{aligned}
 d\tilde{K}_{cc}[\psi, z_c; \zeta] &= \frac{1}{\pi} \int_0^{2\pi} \frac{[\zeta'(\tau)]^\perp \cdot [z_c(t) - z_c(\tau)] + [z_c'(\tau)]^\perp \cdot [\zeta(t) - \zeta(\tau)]}{|z_c(t) - z_c(\tau)|^2} \psi(\tau) d\tau \\
 &\quad - \frac{2}{\pi} \int_0^{2\pi} \frac{[z_c'(\tau)]^\perp \cdot [z_c(t) - z_c(\tau)][z_c(t) - z_c(\tau)] \cdot [\zeta(t) - \zeta(\tau)]}{|z_c(t) - z_c(\tau)|^4} \psi(\tau) d\tau, \\
 d\tilde{K}_{cm}[\psi, z_c; \zeta] &= \frac{1}{\pi} \int_0^{2\pi} \frac{[\zeta'(\tau)]^\perp \cdot [z_m(t) - z_c(\tau)] - [z_c'(\tau)]^\perp \cdot \zeta(\tau)}{|z_m(t) - z_c(\tau)|^2} \psi(\tau) d\tau \\
 &\quad + \frac{2}{\pi} \int_0^{2\pi} \frac{[z_c'(\tau)]^\perp \cdot [z_m(t) - z_c(\tau)][z_m(t) - z_c(\tau)] \cdot \zeta(\tau)}{|z_m(t) - z_c(\tau)|^4} \psi(\tau) d\tau, \\
 d\tilde{K}_{mc}[\psi, z_c; \zeta] &= \frac{1}{\pi} \int_0^{2\pi} \frac{[z_m'(\tau)]^\perp \cdot \zeta(\tau)}{|z_c(t) - z_m(\tau)|^2} \psi(\tau) d\tau \\
 &\quad - \frac{2}{\pi} \int_0^{2\pi} \frac{[z_m'(\tau)]^\perp \cdot [z_c(t) - z_m(\tau)][z_c(t) - z_m(\tau)] \cdot \zeta(\tau)}{|z_c(t) - z_m(\tau)|^4} \psi(\tau) d\tau \quad (3.13)
 \end{aligned}$$

for $t \in [0, 2\pi]$. The kernel of the operator $d\tilde{K}_{cc}$ is smooth with the diagonal values

$$\frac{[z_c'(t)]^\perp \cdot \zeta''(t) + [\zeta'(t)]^\perp \cdot z_c''(t)}{2\pi |z_c'(t)|^2} - \frac{[z_c'(t)]^\perp \cdot z_c''(t) z_c'(t) \cdot \zeta'(t)}{\pi |z_c'(t)|^4}.$$

Given an approximation $z_c, \tilde{\lambda}, \tilde{\mu}$ and $\varphi_l, l = 1, \dots, p$, for a solution of (3.10) and (3.11), then linearizing both equations with respect to all four unknowns leads to the linear equations

$$\begin{aligned}
 &\tilde{S}_{cm} \left((\tilde{\mu} \chi'_l)' - \tilde{\lambda} \chi_l \right) + \tilde{K}_{cm} \chi_l + \tilde{S}_{cm} \left((\beta \varphi'_l)' - \alpha \varphi_l \right) \\
 &+ d\tilde{S}_{cm} \left[(\tilde{\mu} \varphi'_l)' - \tilde{\lambda} \varphi_l, z_c; \zeta \right] + d\tilde{K}_{cm}[\varphi_l, z_c; \zeta] \\
 &= f_l + \tilde{K}_{mms} f_l - \tilde{S}_{mm} g_l - \tilde{S}_{cm} \left((\tilde{\mu} \varphi'_l)' - \tilde{\lambda} \varphi_l \right) - \tilde{K}_{cm} \varphi_l \quad (3.14)
 \end{aligned}$$

and

$$\begin{aligned}
 &\tilde{S}_{cc} \left((\tilde{\mu} \chi'_l)' - \tilde{\lambda} \chi_l \right) - \chi_l + \tilde{K}_{cc} \chi_l + \tilde{S}_{cc} \left((\beta \varphi'_l)' - \alpha \varphi_l \right) \\
 &+ d\tilde{S}_{cc} \left[(\tilde{\mu} \varphi'_l)' - \tilde{\lambda} \varphi_l, z_c; \zeta \right] + d\tilde{K}_{cm}[\varphi_l, z_c; \zeta] \\
 &- d\tilde{K}_{mc}[f_l, z_c; \zeta] + d\tilde{S}_{mc}[g_l, z_c; \zeta] \\
 &= \tilde{K}_{mc} f_l - \tilde{S}_{mc} g_l - \tilde{S}_{cc} \left((\tilde{\mu} \varphi'_l)' - \tilde{\lambda} \varphi_l \right) + \varphi_l - \tilde{K}_{cc} \varphi_l \quad (3.15)
 \end{aligned}$$

that has to be solved for ζ, α, β and $\chi_l, l = 1, \dots, p$, to update the given approximation $z_c, \tilde{\lambda}, \tilde{\mu}$ and $\varphi_l, l = 1, \dots, p$, into $z_c + \zeta, \tilde{\lambda} + \alpha, \tilde{\mu} + \beta$ and $\varphi_l + \chi_l, l = 1, \dots, p$.

Concluding this section, we now can summarize our **inverse algorithm** as follows:

Step A. For an initial approximation $z_c, \tilde{\lambda}, \tilde{\mu}$ for the boundary shape and the impedance functions solve the linear equations (3.11) for initial approximations $\varphi_l, l = 1, \dots, p$. (For the well-posedness of (3.11) we refer to [7, theorem 3.3].)

Step B. Solve the linearized system (3.14)–(3.15) by Tikhonov regularization for ζ , α , β and χ_ℓ , $l = 1, \dots, p$, and replace z_c , $\tilde{\lambda}$, $\tilde{\mu}$ by $z_c + \zeta$, $\tilde{\lambda} + \alpha$, $\tilde{\mu} + \beta$ and φ_ℓ by $\varphi_\ell + \chi_\ell$ for $l = 1, \dots, p$. Repeat this step until some suitable stopping criteria is fulfilled.

Concerning computational costs, in each iteration step B we need to solve p linear integral equations on Γ_c for p up-dates for boundary traces plus the up-dates for the boundary shape and the impedance functions via the least squares procedure for the Tikhonov regularization. Therefore, although we do not solve forward problems in our algorithm, roughly speaking one iteration step B can be viewed to be of the same cost as solving p forward problems.

Before we describe a numerical implementation of this algorithm in more detail and, as a proof of concept, present some numerical examples in the final section of our paper, in the following section we address the injectivity of the linearized system (3.14)–(3.15).

4. Local injectivity

We proceed with four lemmas relating the Fréchet derivatives of the single- and double-layer operators to the boundary traces of the derivatives of certain potentials. For these lemmas we need to assume that Γ_c is of class C^3 to ensure that $\zeta = q [z'_c]^\perp \in C^2[0, 2\pi]$ for a scalar function $q \in C^2[0, 2\pi]$.

Lemma 4.1. For $\varphi \in H_{\text{per}}^2[0, 2\pi]$ and $\zeta \in C^2[0, 2\pi]$ of the form $\zeta = q [z'_c]^\perp$ we have

$$d\tilde{K}_{cc}[\varphi, z_c; \zeta] = 2V_1 \circ z_c + 2[(\text{grad } v_1) \circ z_c] \cdot \zeta \quad (4.1)$$

and

$$d\tilde{K}_{cm}[\varphi, z_c; \zeta] = 2V_1 \circ z_m, \quad (4.2)$$

where

$$\begin{aligned} V_1(x) := & \int_0^{2\pi} \varphi(\tau) \text{grad}_x \left(\text{grad}_x \Phi(x, z_c(\tau)) \cdot [z'_c(\tau)]^\perp \right) \cdot \zeta(\tau) d\tau \\ & - \int_0^{2\pi} \varphi(\tau) \text{grad}_x \Phi(x, z_c(\tau)) \cdot [\zeta'(\tau)]^\perp d\tau \end{aligned} \quad (4.3)$$

and

$$v_1(x) := - \int_0^{2\pi} \varphi(\tau) \text{grad}_x \Phi(x, z_c(\tau)) \cdot [z'_c(\tau)]^\perp d\tau \quad (4.4)$$

for $x \in \mathbb{R}^2 \setminus \Gamma_c$. Both terms on the right-hand side of (4.1) do not have jumps across Γ_c .

Proof. The proof of lemma 4.1 in [8] for the relation (4.1) carries over to this case and is related to the proof of Maue's formula in theorem 7.32 in [18]. Actually, the required partial integrations are less involved since here we integrate over a closed curve and have no troubles with end-point singularities as in the case of an open arc considered in [8]. This also allows the change in the regularity assumptions on φ as compared with those in [8]. The relation (4.1) follows immediately from the representation of $d\tilde{K}_{cm}$ in (3.13). \square

Lemma 4.2. For $\varphi \in H_{\text{per}}^2[0, 2\pi]$ we set

$$\eta := (\tilde{\mu}\varphi)' - \tilde{\lambda}\varphi. \quad (4.5)$$

Then

$$d\tilde{S}_{cc}[\eta, z_c; \zeta] = 2V_2 \circ z_c + 2[(\text{grad } v_2) \circ z_c] \cdot \zeta \quad (4.6)$$

and

$$d\tilde{S}_{cm}[\eta, z_c; \zeta] = 2V_2 \circ z_m \quad (4.7)$$

where

$$V_2(x) := -\int_0^{2\pi} \eta(\tau) \text{grad}_x \Phi(x, z_c(\tau)) \cdot \zeta(\tau) \, d\tau \quad (4.8)$$

and

$$v_2(x) := \int_0^{2\pi} \eta(\tau) \Phi(x, z_c(\tau)) \, d\tau \quad (4.9)$$

for $x \in \mathbb{R}^2 \setminus \Gamma_c$.

Proof. This is an immediate consequence of the jump relations for single- and double-layer potentials and the representation of the Fréchet derivatives of the single-layer operators from (3.12). The jumps of the two terms on the right-hand side of (4.6) have opposite signs. \square

Lemma 4.3. For $f \in H_{\text{per}}^{1/2}[0, 2\pi]$ and $g \in H_{\text{per}}^{-1/2}[0, 2\pi]$ we have

$$d\tilde{S}_{mc}[g, z_c; \zeta] - d\tilde{K}_{mc}[f, z_c; \zeta] = 2[(\text{grad } w) \circ z_c] \cdot \zeta, \quad (4.10)$$

where

$$w(x) := \frac{1}{2\pi} \int_0^{2\pi} \left\{ \ln \frac{1}{|x - z_m(\tau)|} g(\tau) - \frac{[z'_j(\tau)]^\perp \cdot [x - z_m(\tau)]}{|x - z_m(\tau)|^2} f(\tau) \right\} d\tau \quad (4.11)$$

for $x \in \mathbb{R}^2 \setminus \Gamma_c$.

Proof. This is obvious from (3.12) and (3.13). \square

Lemma 4.4. Under the assumptions of lemma 4.1 we can transform

$$V_1(x) = -\int_0^{2\pi} (q(\tau)\varphi'(\tau))' \Phi(x, z_c(\tau)) \, d\tau, \quad x \in \mathbb{R}^2 \setminus \Gamma_c. \quad (4.12)$$

Proof. As in the proof for lemma 4.3 in [8], it can be shown that

$$V_1(x) = \int_0^{2\pi} q(\tau)\varphi'(\tau) \frac{d}{d\tau} \Phi(x, z_c(\tau)) d\tau, \quad x \in \mathbb{R}^2 \setminus \Gamma_c.$$

From this (4.12) follows by partial integration. \square

We are now ready for the main result of this section by deriving an ordinary differential equation of order four for solutions of the homogeneous form of the linearized integral equations (3.14) and (3.15).

Theorem 4.5. *Let u be solution to (1.1) and (1.2) with Cauchy data (f, g) , which implies that $z_c, \tilde{\lambda}$ and $\tilde{\mu}$ and $\varphi = u \circ z_c$ satisfy the integral equations (3.10) and (3.11). Then for any solution $\zeta = q[z_c']^\perp \in C^2[0, 2\pi]$, $\alpha \in C^1[0, 2\pi]$, $\beta \in C^1[0, 2\pi]$ and $\chi \in H^2[0, 2\pi]$ to the homogeneous system*

$$\begin{aligned} & \tilde{S}_{cm}((\tilde{\mu}\chi)' - \tilde{\lambda}\chi) + \tilde{K}_{cm}\chi + \tilde{S}_{cm}((\beta\varphi)' - \alpha\varphi) \\ & + d\tilde{S}_{cm}[(\tilde{\mu}\varphi)' - \tilde{\lambda}\varphi, z_c; \zeta] + d\tilde{K}_{cm}[\varphi, z_c; \zeta] = 0 \end{aligned} \quad (4.13)$$

and

$$\begin{aligned} & \tilde{S}_{cc}((\tilde{\mu}\chi)' - \tilde{\lambda}\chi) - \chi + \tilde{K}_{cc}\chi + \tilde{S}_{cc}((\beta\varphi)' - \alpha\varphi) \\ & + d\tilde{S}_{cc}[(\tilde{\mu}\varphi)' - \tilde{\lambda}\varphi, z_c; \zeta] + d\tilde{K}_{cm}[\varphi, z_c; \zeta] \\ & - d\tilde{K}_{mc}[f, z_c; \zeta] + d\tilde{S}_{mc}[g, z_c; \zeta] = 0 \end{aligned} \quad (4.14)$$

we have that

$$\chi = ((\tilde{\mu}\varphi)' - \tilde{\lambda}\varphi)q \quad (4.15)$$

and

$$(q\varphi)' - (\tilde{\mu}\chi)' + \tilde{\lambda}\chi - (\beta\varphi)' + \alpha\varphi = 0. \quad (4.16)$$

Proof. In addition to the harmonic functions V_1, V_2, v_1, v_2 and w introduced in the preceding lemmas we further define

$$W_1(x) := -\int_0^{2\pi} \chi(\tau) \operatorname{grad}_x \Phi(x, z_c(\tau)) \cdot [z_c'(\tau)]^\perp d\tau,$$

$$W_2(x) := \int_0^{2\pi} ((\tilde{\mu}\chi)' - \tilde{\lambda}\chi)(\tau) \Phi(x, z_c(\tau)) d\tau,$$

$$W_3(x) := \int_0^{2\pi} ((\beta\varphi)' - \alpha\varphi)(\tau) \Phi(x, z_c(\tau)) d\tau$$

for $x \in \mathbb{R}^2 \setminus \Gamma_c$ and set

$$V := W_1 + V_1 + W_2 + V_2 + W_3.$$

By Green's integral formula (3.3) we have that

$$v_1 + v_2 + w = \begin{cases} u & \text{in } \Omega, \\ 0 & \text{in } \mathbb{R}^2 \setminus \Omega. \end{cases} \quad (4.17)$$

Via (3.7), (3.8), (4.1) and (4.6) the homogeneous equation (4.13) implies that

$$V = 0 \quad \text{on } \Gamma_m. \quad (4.18)$$

From this, due to our geometric assumption on the domain Ω , proceeding as in the proof of theorem 3.16 in [17], it can be concluded that $V = 0$ in $\mathbb{R}^2 \setminus \overline{\Omega}_m$. Then analyticity of V implies that $V = 0$ in $\mathbb{R}^2 \setminus \overline{\Omega}_c$.

Using (4.1) and (4.6), from the homogeneous equations (4.14) and (4.17) it can be seen that the boundary values of V by approaching Γ_c from inside Ω_c satisfy

$$V = 0 \quad \text{on } \Gamma_c \quad (4.19)$$

and those obtained from inside Ω satisfy

$$V \circ z_c + 2\chi + 2\zeta \cdot \text{grad } u \circ z_c = 0. \quad (4.20)$$

From (4.19) we have that $V = 0$ in Ω_c , that is, altogether $V = 0$ in $\mathbb{R}^2 \setminus \Gamma_c$. Hence, in view in view of $\zeta = q[z'_c]^\perp = q[z'_c] \circ z$, using the generalized impedance boundary condition for u we obtain (4.15) from (4.20).

Again from $V = 0$ in $\mathbb{R}^2 \setminus \Gamma_c$, in view of the definitions of the potentials summing up in V , using lemmas 4.1 and 4.4 and the jump relations for single- and double-layer potentials we obtain (4.16). \square

Corollary 4.6. *Under the assumptions of theorem 4.5, using $p = 5$ linearly independent Cauchy pairs in (3.14) and (3.15) ensures injectivity.*

Proof. Assume that q, α, β together with χ_1, \dots, χ_5 solve (3.14) and (3.15) with right-hand sides equal to zero for $p = 5$. Inserting (4.15) into (4.16) we obtain a fourth order linear differential equation with leading coefficient $q\tilde{\mu}^2$ that is satisfied for the corresponding $\varphi_\ell = u_\ell \circ z_c$ for $\ell = 1, \dots, 5$. By the homogeneous generalized impedance condition and Holmgren's uniqueness theorem, the linear independence of the Dirichlet data f_1, \dots, f_5 implies linear independence of $\varphi_1, \dots, \varphi_5$. Since a fourth order linear differential equation with non-vanishing leading coefficient admits only four linearly independent solution we must have $q\tilde{\mu}^2 = 0$ in $[0, 2\pi]$ and the assumption $\mu > 0$ implies that $q = 0$ in $[0, 2\pi]$. Then from (4.15) it follows that $\chi = 0$ in $[0, 2\pi]$ and, finally, from (4.16) we obtain $\alpha = \beta = 0$ in $[0, 2\pi]$. \square

We want to show that $p = 5$ is optimal in the statement of corollary 4.6 by constructing an example where four linearly independent Cauchy pairs give rise to non-trivial solutions of (3.14) and (3.15). To this end let Ω be the annulus bounded by $\Gamma_m := \{x : |x| = R\}$ and $\Gamma_c := \{x : |x| = \rho < R\}$. We consider the complex valued function

$$u(r, \theta) = \left(\frac{r^n}{\rho^n} + b_n \frac{\rho^n}{r^n} \right) e^{in\theta} \quad (4.21)$$

for $n \in \mathbb{N}$ and $b_n \in \mathbb{R}$ in polar coordinates (r, θ) . The generalized impedance boundary condition on the circle $\rho < R$ with constant $\mu > 0$ and $\lambda > 0$ is satisfied provided the constant b_n is chosen such that

$$b_n = \frac{n\rho - \mu n^2 - \lambda\rho^2}{n\rho + \mu n^2 + \lambda\rho^2}. \quad (4.22)$$

In particular, for the input functions in (3.14) and (3.15) we have

$$q_n = (1 + b_n)e_n, \quad f_n = \left(\frac{R^n}{\rho^n} + b_n \frac{\rho^n}{R^n} \right) e_n, \quad g_n = \left(n \frac{R^n}{\rho^n} - nb_n \frac{\rho^n}{R^n} \right) e_n \quad (4.23)$$

where we have set $e_n(t) := e^{int}$. (Note that in (3.14) and (3.15) we understand g_n as the normal derivative multiplied by arc length.)

Applying Green's formula to the harmonic functions $r^{\pm n} e^{in\theta}$ for $n \in \mathbb{N}$ we obtain that

$$S_{cc}(n\rho^n e_n) - K_{cc}(\rho^n e_n) = \rho^n e_n, \quad S_{cc}(-n\rho^{-n} e_n) - K_{cc}(\rho^{-n} e_n) = -\rho^{-n} e_n$$

and consequently

$$S_{cc}e_n = \frac{1}{n} e_n, \quad K_{cc}e_n = 0. \quad (4.24)$$

(Note that the parameterized single-layer potentials do not contain the arc length.) Analogously from

$$S_{cm}(n\rho^n e_n) - K_{cm}(\rho^n e_n) = 0, \quad S_{cm}(-n\rho^{-n} e_n) - K_{cm}(\rho^{-n} e_n) = -2R^{-n} e_n$$

we find

$$S_{cm}e_n = \frac{\rho^n}{nR^n} e_n, \quad K_{cm}e_n = \frac{\rho^n}{R^n} e_n, \quad (4.25)$$

and from

$$S_{mc}(nR^n e_n) - K_{mc}(R^n e_n) = 2\rho^n e_n, \quad S_{mc}(-nR^{-n} e_n) - K_{mc}(R^{-n} e_n) = 0$$

we obtain

$$S_{mc}e_n = \frac{\rho^n}{nR^n} e_n, \quad K_{mc}e_n = -\frac{\rho^n}{R^n} e_n. \quad (4.26)$$

Noting that $\tilde{\lambda} = \rho\lambda$ and $\tilde{\mu} = \mu/\rho$ we put (4.24)–(4.26) together and conclude that looking for a solution of (3.14) and (3.15) with constants q, α, β and $\chi_n = \xi_n e_n$ is equivalent to solving

$$\frac{1}{\rho n} (\mu n^2 + \lambda\rho^2) \xi_n - \xi_n + \frac{1}{n} (\beta n^2 + \alpha)(1 + b_n) + \frac{1}{\rho^2} (\mu n^2 + \lambda\rho^2 + \rho n)(1 + b_n)q = 0$$

and

$$-\frac{1}{\rho n} (\mu n^2 + \lambda\rho^2) \xi_n - \xi_n - \frac{1}{n} (\beta n^2 + \alpha)(1 + b_n) + \frac{2n}{\rho} q = 0.$$

Scaling the solution by setting $q = 1$ and adding the two equations, in view of (4.23) we see that in turn they are equivalent to

$$\xi_n = \frac{2n}{\rho} \quad (4.27)$$

and

$$(\beta n^2 + \alpha)(1 + b_n) + \frac{4}{\rho^2} (\mu n^2 + \lambda \rho^2) = 0. \quad (4.28)$$

We now pick two different $n_1, n_2 \in \mathbb{N}$ and solve the two-by-two system

$$(\beta n_j^2 + \alpha)(1 + b_{n_j}) + \frac{4}{\rho^2} (\mu n_j^2 + \lambda \rho^2) = 0, \quad j = 1, 2,$$

for α and β and together with $q = 1$ and $\xi_{n_j} = 2n_j/\rho$ the real and imaginary parts provide a non-trivial solution of (3.14) and (3.15) for four linearly independent Cauchy pairs.

5. Numerical examples

As proof of concept rather than a documentation of a fully developed code, in this final section we present some numerical examples. For these the data were obtained by the integral equations presented in [7]. We note that these boundary integral equations for creating the data are obtained by a potential approach whereas the integral equations in the inverse algorithm are based on Green's formula and thus committing an inverse crime is avoided.

In principle, the parameterization of the update ζ obtained from (3.14) and (3.15) is not unique. To cope with this ambiguity, we use star-like parameterizations of the form

$$z_c(t) = r(t)(\cos t, \sin t), \quad 0 \leq t \leq 2\pi, \quad (5.1)$$

with a non-negative function r representing the radial distance of Γ_c from the origin. Consequently, the perturbations are of the form

$$\zeta(t) = q(t)(\cos t, \sin t), \quad 0 \leq t \leq 2\pi, \quad (5.2)$$

with a real function q . In the approximations we assume r and its update q to have the form of a trigonometric polynomial of degree J_{shape} . In all our examples we choose $J_{\text{shape}} = 6$.

For all examples the exact impedance functions are given by

$$\lambda(z_c(t)) = \frac{0.5}{1 + 0.3 \sin t} \quad \text{and} \quad \mu(z_c(t)) = \frac{1}{1 + 0.2 \cos 2t} \quad (5.3)$$

for $t \in [0, 2\pi]$. In the inverse algorithm, in all examples we approximated both impedance functions $\lambda \circ z_c$ and $\mu \circ z_c$ by trigonometric polynomials of degree J_{imp} . Correspondingly, in (3.14)–(3.15) we approximated the impedance update functions for $\tilde{\lambda}$ and $\tilde{\mu}$ in the form $\alpha = \hat{\alpha}/|z_c'|$ and $\beta = \hat{\beta}/|z_c'|$ with trigonometric polynomials $\hat{\alpha}$ and $\hat{\beta}$ of degree J_{imp} . Then $\hat{\alpha}$ and $\hat{\beta}$ serve as update functions for λ and μ , respectively. In all our examples we used $J_{\text{imp}} = 3$.

For the numerical implementation of the starting step A we discretized the linear equations (3.11) analogous to the method described in [7] for the direct problem with $2n$ equidistant collocation and quadrature points $t_j = j\pi/n$, $j = 1, \dots, 2n$. For the iteration step B we collocated the system (3.14)–(3.15) at the points t_j , $j = 1, \dots, 2n$, and solved by Tikhonov regularization for the nodal values $\varphi_\ell(t_j)$, $\ell = 1, \dots, p$, $j = 1, \dots, 2n$, and the Fourier coefficients of the update trigonometric polynomials q , $\hat{\alpha}$ and $\hat{\beta}$.

The measurement curve Γ_m is the circle with the representation

$$z_m(t) = 0.9(\cos t, \sin t), \quad t \in [0, 2\pi],$$

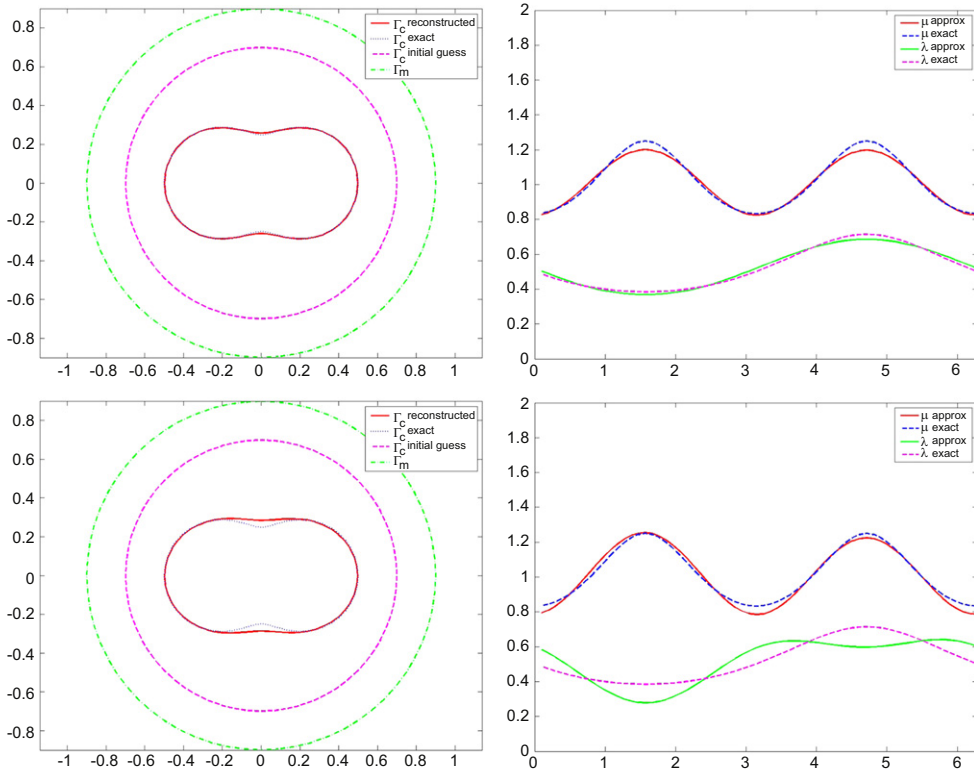


Figure 1. Reconstruction of (5.4) for exact data (above) and 2% noise (below).

where the factor 0.9 is chosen to satisfy the geometric condition introduced on p. 6. We used five Cauchy pairs with Dirichlet data

$$f_\ell(z_m(t)) = \cos \ell t, \quad \ell = 0, 1, 2, \quad f_{\ell+2}(z_m(t)) = \sin \ell t, \quad \ell = 1, 2.$$

The number of collocation and quadrature points is $2n = 64$ on each curve.

The four regularization parameters and the stopping rule for the iteration are chosen by trial and error. However, to illustrate the feasibility and the stability of our method we used the same regularization parameters in all examples. Depending on the m th iteration step, for exact data the regularization parameters for an H^2 penalization with respect to all four unknowns are chosen as $\alpha_q = 0.8^m$ for the shape function, $\alpha_\lambda = \alpha_\mu = 0.1 \cdot 0.8^m$ for the impedance functions and $\alpha_\chi = 10^{-9}$ for the Dirichlet trace. For noisy data these parameters are $\alpha_q = 0.95^m$, $\alpha_\lambda = \alpha_\mu = 0.1 \cdot 0.95^m$ and $\alpha_\chi = 10^{-9}$. For the perturbed data, random noise is added point-wise and the relative error is with respect to the L^2 norm. The iterations are started with an initial guess given by a circle of radius 0.7 centered at the origin and constant values $\lambda_0 = \mu_0 = 0.8$. They are stopped after 30 iterations for exact data and 25 iterations for noisy data.

The three shapes to be reconstructed are a peanut-shaped curve

$$z_c(t) = 0.5\sqrt{\cos^2 + 0.25 \sin^2 t}(\cos t, \sin t), \tag{5.4}$$

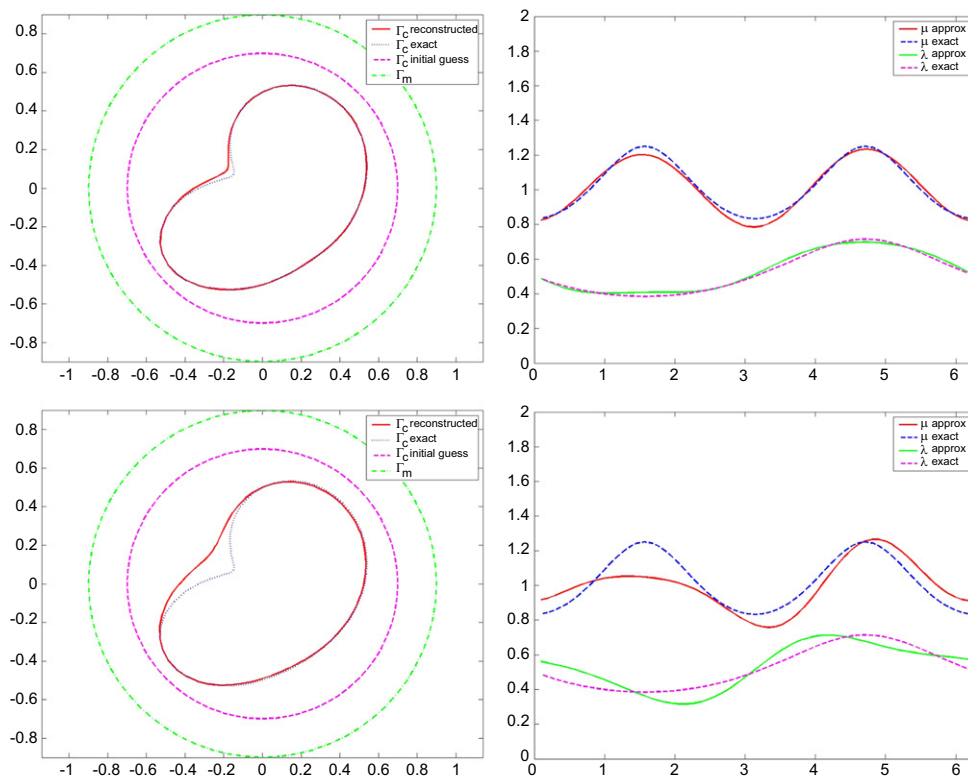


Figure 2. Reconstruction of (5.5) for exact data (above) and 2% noise (below).

an apple-shape curve

$$z_c(t) = \frac{0.5 + 0.4 \cos t + 0.1 \cos 2t}{1 + 0.7 \cos t} (\cos t, \sin t) \quad (5.5)$$

and a kite-shaped curve

$$z_c(t) = (-0.2 + 0.4 \cos t + 0.2 \cos 2t, 0.4 \sin t) \quad (5.6)$$

for $0 \leq t \leq 2\pi$. Note that neither the boundary curves nor the impedance functions belong to the corresponding approximation spaces.

In figures 1–3 the exact Γ_c is given as dotted (blue) curve and the reconstruction as full (red) curve. The measurement curve Γ_m is dashed-dotted (green) and the initial guess dashed (magenta). The exact μ is given as dashed (blue) curve and the reconstruction as full (red) curve, the exact λ is dashed (magenta) and the reconstruction full (green).

In general, we observed that the algorithm sort of first tries to find the shape and only later on improves on the reconstruction of the impedance function which explains the rather large iteration number for reasonable accuracy.

Acknowledgments

Part of this research was done while RK was visiting the University of Delaware. The support and the hospitality are gratefully acknowledged. The research of FC is supported in part by

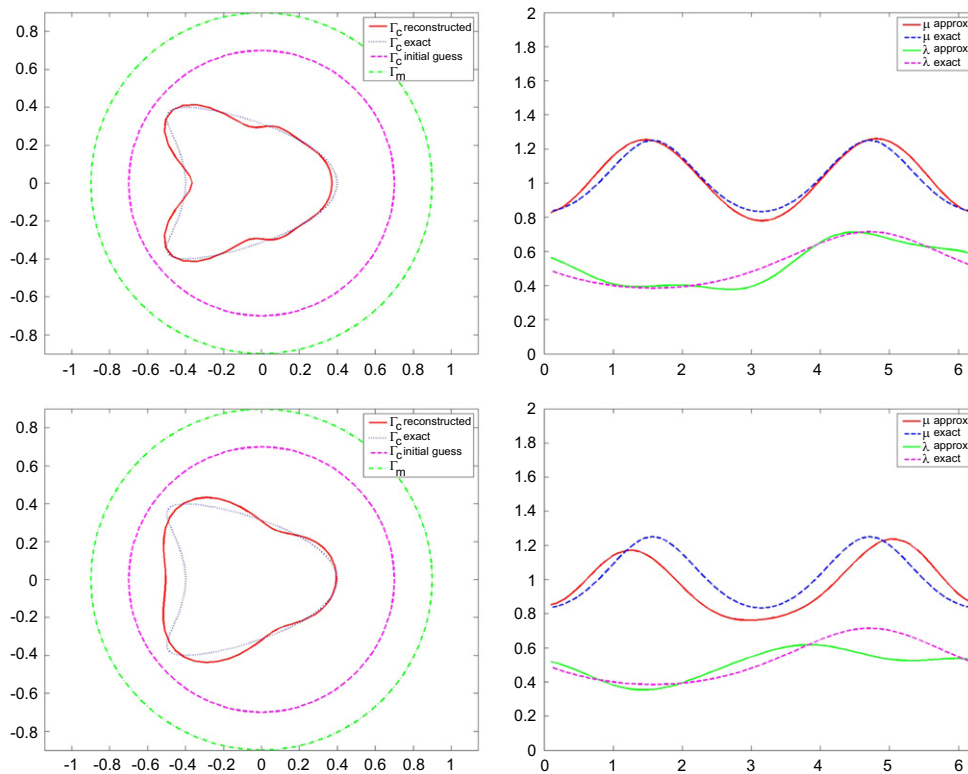


Figure 3. Reconstruction of (5.6) for exact data (above) and 2% noise (below).

the AFOSR grant FA9550-13-1-0199. The research of YH is supported by the NSFC grant 91330109.

References

- [1] Aslanyrek G, Haddar H and Sahintürk H 2011 Generalized impedance boundary conditions for thin dielectric coatings with variable thickness *Wave Motion* **48** 680–99
- [2] Bacchelli V 2009 Uniqueness for the determination of unknown boundary and impedance with the homogeneous Robin condition *Inverse Problems* **25** 015004
- [3] Bourgeois L and Haddar H 2010 Identification of generalized impedance boundary conditions in inverse scattering problems *Inverse Probl. Imag.* **4** 19–38
- [4] Bourgeois L, Chaulet N and Haddar H 2011 Stable reconstruction of generalized impedance boundary conditions *Inverse Problems* **27** 095002
- [5] Bourgeois L, Chaulet N and Haddar H 2012 On simultaneous identification of a scatterer and its generalized impedance boundary condition *SIAM J. Sci. Comput.* **34** 1824–48
- [6] Cakoni F and Kress R 2007 Integral equations for inverse problems in corrosion detection from partial Cauchy data *Inverse Probl. Imag.* **1** 229–45
- [7] Cakoni F and Kress R 2013 Integral equation methods for the inverse obstacle problem with generalized impedance boundary condition *Inverse Problems* **29** 015005
- [8] Cakoni F, Kress R and Schuft C 2010 Integral equations for shape and impedance reconstruction in corrosion detection *Inverse Problems* **26** 095012
- [9] Cakoni F, Kress R and Schuft C 2010 Simultaneous reconstruction of shape and impedance in corrosion detection *J. Methods Appl. Anal.* **17** 357–78

- [10] Colton D and Kress R 2012 *Inverse Acoustic and Electromagnetic Scattering Theory* 3rd edn (New York: Springer)
- [11] Duruflé M, Haddar H and Joly J 2006 Higher order generalized impedance boundary conditions in electromagnetic scattering problems *C. R. Phys.* **7** 533–42
- [12] Evans L 1998 *Partial Differential Equations* (Providence, RI: American Mathematical Society)
- [13] Haddar H and Joly J 2002 Stability of thin layer approximation of electromagnetic waves scattering by linear and nonlinear coatings *J. Comput. Appl. Math.* **143** 201–36
- [14] Haddar H, Joly J and Nguyen H-M 2005 Generalized impedance boundary conditions for scattering by strongly absorbing obstacles: the scalar case *Math. Models Methods Appl. Sci.* **15** 1273–300
- [15] Johansson T and Sleeman B 2007 Reconstruction of an acoustically sound-soft obstacle from one incident field and the far-field pattern *IMA J. Appl. Math.* **72** 96–112
- [16] Kirsch A 1989 Surface gradients and continuity properties for some integral operators in classical scattering theory *Math. Methods Appl. Sci.* **11** 789–804
- [17] Kirsch A 2011 *An Introduction to the Mathematical Theory of Inverse Problems* 2nd edn (New York: Springer)
- [18] Kress R 2014 *Integral Equations* 3rd edn (New York: Springer)
- [19] Kress R 2014 A collocation method for a hypersingular boundary integral equation via trigonometric differentiation *J. Integral Equ. Appl.* **26** 197–213
- [20] Kress R and Rundell W 2005 Nonlinear integral equations and the iterative solution for an inverse boundary value problem *Inverse Problems* **21** 1207–23
- [21] Rundell W 2008 Recovering an obstacle and its impedance from Cauchy data *Inverse Problems* **24** 045003